Hydrogen Bonding and Dynamic Crossover in Polyamide-66: A Molecular Dynamics Simulation Study

Hossein Ali Karimi-Varzaneh,* Paola Carbone,† and Florian Müller-Plathe

Eduard-Zintl-Institut für Anorganische and Physikalische Chemie, Technische Universität Darmstadt, Petersenstrasse 20, D-64287 Darmstadt, Germany

Received May 13, 2008; Revised Manuscript Received July 22, 2008

ABSTRACT: Using molecular dynamics simulations, we study the hydrogen bond dynamics and thermodynamics of the bulk of polyamide-66 over a broad temperature range (300−600 K). We show that different dynamic properties (the structure relaxation time, the orientational time correlation function of the amide groups, and the self-diffusion coefficient) of unentangled polyamide-66 undertake a crossover transition in the same small temperature range (∼ 413 K) above the experimental glass transition temperature (350 K). The data can be fitted to a Vogel−Fulcher−Tammann law when $T > 413$ K and to an Arrhenius equation when $T < 413$ K. Our results show that the global dynamics of polyamide-66 is intimately related to the relaxation of the hydrogen bond network formed among the amide groups. The presence of a dynamic crossover at a temperature slightly higher than the glass transition one is in agreement with the more recent experimental data and glass theories.

Introduction

Nylons are some of the commercially most important engineering polymers. They are used for textiles and carpets and also, in bulk, as an engineering plastic.[1] The recent developments in nylon are based on the structure and mobility properties. Via investigation of the influence of the structure on chain mobility, it is possible to understand the correlation between structural features and polymer properties. Nylons are specified as either PA-*x* or PA-*xy*, where PA identifies nylons as a polyamide and *x* and *y* represent the number of carbon atoms between successive nitrogen atoms. Homologous series of nylons provide an opportunity to study in detail the role of hydrogen bonding in mobility, hydration, chain folding, crystallization, and deformation. Among dual-numbered nylons, PA-66 is the most important.

In polyamides, nearly all the amide groups that separate a sequence of methylene groups are hydrogen-bonded.[2] This large number of hydrogen bonds forms an extended three-dimensional network whose destruction influences several properties of the material such as the glass transition temperature and the melting point. For these reasons, understanding the thermal mechanical properties of polyamides by studying the thermal stability of hydrogen bonds was a popular topic in previous research.[2−6] The mobility of different parts of PA-66 has been studied experimentally with nuclear magnetic resonance (NMR) methods,[7] quasi-elastic neutron scattering,[8] and Fourier-transform infrared (FTIR) spectroscopy.[9] In these experiments, it has been shown that in PA-66 crystals the amide hydrogen bonds (HBs) are relatively immobile at all temperatures below 503 K (the melting point is 533 K). In particular, temperature-resolved FTIR spectroscopy is the usual methodology for investigating the status of hydrogen bonding at different temperatures. Schroeder and Cooper[6] developed a procedure for estimating the thermodynamic parameters associated with hydrogen bond dissociation in polyamides from the total area change of the N−H stretching region induced by heat. The essential assumption is that the absorption coefficient of N−H stretching does not vary significantly with temperature. However, Skrovanek and co-workers[10,11] found that actually the absorption coefficient of N−H stretching depends strongly on temperature and the fraction of nonbonded N−H groups, as estimated from FTIR spectroscopy, is overestimated in the experiments. Thus, the experimental methods investigate HB dynamics only indirectly, and they can be interpreted in an only qualitative way.[9]

On the other side, molecular dynamics (MD) simulations can provide quantitative information about HB dynamics with atomistic resolution.[12−15] The factors influencing the dynamics can be obtained from MD trajectories by calculating different HB time correlation functions, as proposed first by Stillinger[16,17] and developed further by Luzar and Chandler.[12]

In this work, using molecular dynamics simulations, we analyze in detail the effect of temperature on the local and global dynamics of unentangled PA-66. The local dynamics are investigated mainly by looking at the HB dynamics, calculating their structure relaxation time and lifetime by means of specific correlation functions. The influence of the relaxation of the HB network on the global dynamics of the polymer is also analyzed. Moreover, the study of the structure relaxation time and the self-diffusion coefficient at different temperatures will also allow us to test the more recent theories developed to describe the physical nature of polymer glasses.[18,19] In fact, polyamides, like other materials, when submitted to a cooling from high temperatures pass through several phase transitions, among which the most important is the glass transition. The origin (thermodynamic or kinetic) of the glass transition and the consequent structural changes occurring at the molecular level are still under investigation. Previously, theory predicted that the properties of glasses or supercooled liquids at low temperatures (far below the glass transition one) could be reliably extrapolated from the high-temperature equilibrium ones.[20,21] In fact, it was generally accepted that most materials exhibit a non-Arrhenius behavior. For example, the diffusion coefficient and viscosity were often described with only one temperature law (the so-called Vogel−Fulcher) in the entire range of temperature. However, recent developments in the theory and new experiments have shown that as the conventional glass transition temperature (T_g) is approached the temperature dependence of the global (diffusion coefficient and viscosity) and local dynamic properties continuously changes from the typical Vogel−Fulcher−Tammann form to the Arrhenius

* To whom correspondence should be addressed. E-mail: h.karimi@theo.chemie.tu-darmstadt.de. Telephone: +49-6151-16-3146. Fax: +49-6151-16-6526.

† Current address: School of Chemical Engineering and Analytical Science, The University of Manchester, Sackville Street, Manchester, M60 1QD, UK.

10.1021/ma8010685 CCC: $40.75
Published on Web 09/10/2008

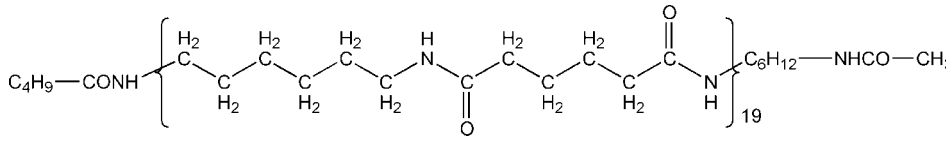

Figure 1. Structure of the polyamide chains employed in simulations.

form.[19,22−24] The change in the temperature dependence of the dynamic properties near the conventional T_g demonstrates the poor reliability of the practice of extrapolating high-temperature properties to low temperatures. Therefore, it is of interest to investigate the problem of the temperature dependence of the dynamic properties using a computational approach. Our simulation results can indeed provide an interesting insight into the temperature dependence of the local and global dynamics and their interdependence in supercooled PA-66. We will compare our results with the most recent glass theories and with experiments conducted with several polymeric systems.

Model and Simulation Details

Twenty-four chains of PA-66 each composed of 20 chemical repeat units, containing 40 amide groups and terminated by ethyl and butyl groups (Figure 1), were investigated by means of molecular dynamics (MD) simulations at different temperatures. Each chain had a molecular weight of around 4540 g/mol, which is just below the experimental entanglement molecular weight (4700 g/mol).[25] The atomistic force field and the initial coordinates of PA-66 were taken from Goudeau et al.;[26] all details concerning the simulations can be found therein. Here, we summarize only the main parameters which define the MD simulations. Temperature and pressure were controlled using the weak coupling scheme introduced by Berendsen[27] (with $\tau_T = 0.2$ ps, $\tau_P = 5$ ps, and an isothermal compressibility of 10^{-6} kPa^{-1}). All simulations were performed at atmospheric pressure. The equation of motion was integrated with a time step of 2 fs. A Verlet neighbor list with a pair cutoff of 1.0 nm was used and updated by a link-cell scheme every 30 steps. Bond constraints were maintained to a relative tolerance of 10^{-6} by the SHAKE procedure.[28,29] All calculations were performed with YASP.[30]

The system was studied at 11 different temperatures (from 300 to 500 K in increments of 25 K and from 500 to 600 K in increments of 50 K) ranging from below to well above the experimental glass transition temperature (350 K).[31] The system was equilibrated for more than 60 ns at low temperatures (<400 K) and for ~40 ns at high temperatures (>400 K). To determine how the system relaxes at different temperatures, we calculated the orientation time-autocorrelation function (OACF) $\langle \mathbf{u}(t)\mathbf{u}(0)\rangle$ for unit vectors **u** along the C−O and N−H bonds of the amide groups. Figure 2 shows the OACF calculated for the amide groups (C−O and N−H bond vectors) at four temperatures. The figure shows that the bond vectors decorrelate fast at high temperatures while they do not decay in the long time in the glassy phase (300 K). To determine if we had achieved a satisfactory relaxed configuration also at low temperatures, we split the simulation box into eight cells (by dividing the box size by two in every direction) and calculated the density in each cell during the simulations. Figure 3 shows the variation in density for three cells (cells with the highest, lowest, and the most typical density) versus time. We still found a fluctuation in the density of up to 2% in different cells after 60 ns, because of the small size of the cells, but the average density (1.1 g/cm^3) in different parts of the simulation box was the same as the experimental value at room temperature (1.07−1.1 g/cm^3).[32] Our system was, thus, homogeneous. This homogeneity even at a low temperature (300 K) meant that our system was globally well equilibrated.

Results and Discussion

Static Properties of Hydrogen Bonds. The amide−amide hydrogen bond (HB) interactions were analyzed at 11 different

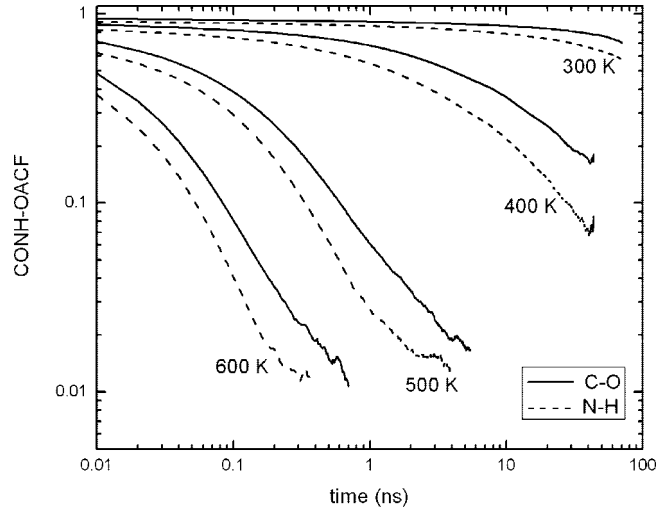

Figure 2. Orientation autocorrelation function for amide groups (C−O and N−H bond vectors) at 300, 400, 500, and 600 K. Solid lines represent the autocorrelation function for C−O bond vectors, and dashed lines correspond to the autocorrelation function for N−H bond vectors at every temperature.

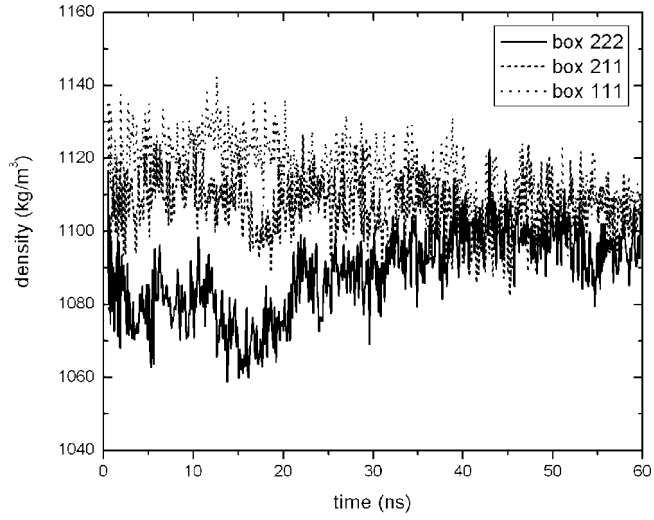

Figure 3. Density variations for subcells with the highest (···), lowest (—), and most typical (---) density vs time. The numbers for every cell (222, 211, and 111) correspond to the position of the subcell in the complete simulation box.

temperatures between 300 and 600 K. The amide N−H group was considered the donor and the amide oxygen the acceptor. The main structural property distinguishing the HBs from the van der Waals interaction is their preference for linearity. To consider the angular preference of HBs, we plotted the N−H···O bond angle (θ) against the H···O distance (d) at 300 K (Figure 4). The plot contains all contacts found in the system with $d < 0.4$ nm regardless of the angle. There are densely populated clusters of data points at short distances and almost linear angles. The shortest distances occur at relatively linear angles (with θ between 150° and 180°), whereas longer bonds are observed with a larger angular range (with θ between 60° and 150°). The plot is unpopulated for distances of <0.175

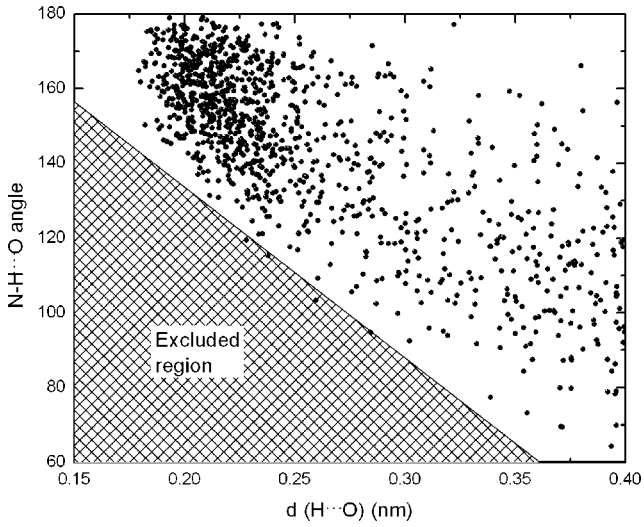

Figure 4. Amide−amide hydrogen bonds. Correlation of the N−H···O bond angle and the H···O distance at 300 K.

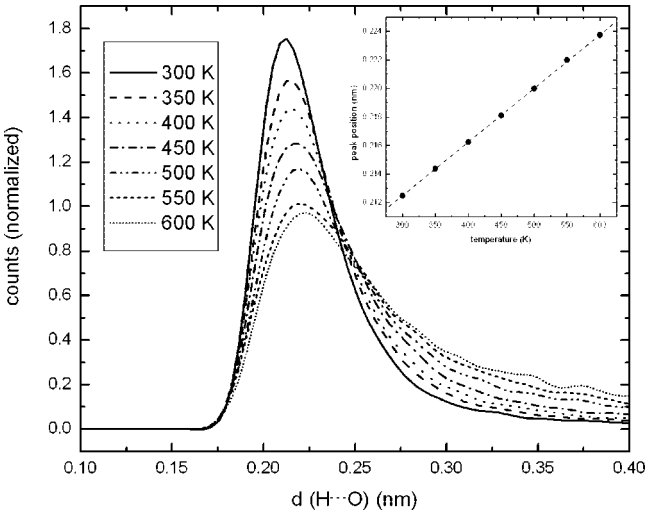

Figure 5. Distribution of the H···O distances for fairly linear hydrogen bonds with $\theta_{N-H\cdots O} > 130°$. This histogram contains data from a horizontal slice ($180° > \theta > 130°$) of Figure 4 at different temperatures. The inset shows the temperature dependence of the peak maximum. The dashed line is the linear fit through the points.

nm, because exchange repulsion prevents shorter distances. In Figure 4, a line limiting the configurations not populated is drawn; it represents the extreme limit of HB bending, which can be considered as an effect of the repulsions between atoms of the amide groups included in the HB.[33]

To study the effect of temperature on the HB length, we plotted the distribution of the H···O distance d for $\theta_{N-H\cdots O} > 130°$ (Figure 5). The distribution of the H···O distance for linear HBs ($\theta_{N-H\cdots O} > 130°$) has a distinct maximum around 0.218 nm at different temperatures. With an increase in temperature, the maximum peak of the distribution of the H···O distance shifts linearly to distances of >0.212 and >0.224 nm for 300 and 600 K, respectively (inset of Figure 5), showing a weakening of the interaction between the hydrogen and the oxygen with an increase in temperature. For high temperatures, the distribution does not fall to zero at long distances but fades into the continuum of random contacts. With an increase in temperature, the distribution of a short H···O distance (around 0.218 nm) decreases and the probability of random contacts at longer distances increases (Figure 5).

Generally, either a geometric[34] or an energetic[14] criterion is used to define a HB. On the basis of the results in the previous

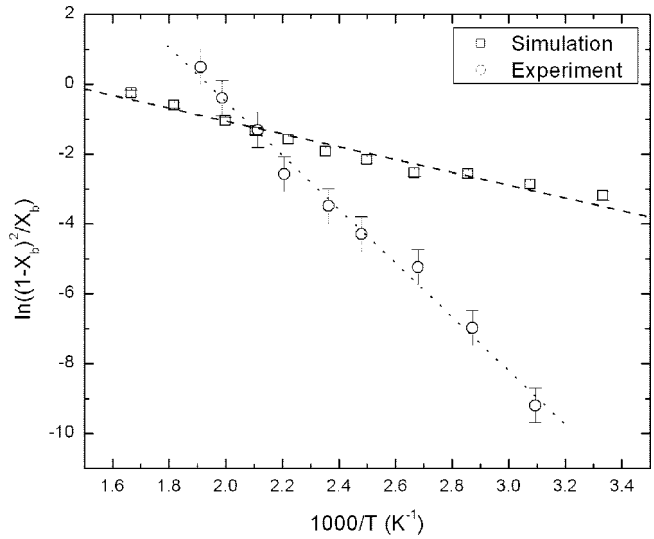

Figure 6. van't Hoff plot of the hydrogen bond dissociation equilibrium in the simulation and the experiment.[3] The dashed and dotted lines are linear fits through the simulation and the experiment points, respectively.

paragraph, in this work the HBs were defined according to a geometric criterion. The distance between the hydrogen of the donor group and the acceptor O has to be <0.297 nm[3] and the donor−hydrogen−acceptor angle >130°.[26]

To calculate the enthalpy (ΔH) of HB breaking, we adopted the model proposed by Schroeder and Cooper[6] which relates ΔH to the bonded amide fraction (X_b). The equilibrium between the hydrogen-bonded and nonbonded amides can be represented by

$$(\mathrm{NH\cdots O{=}C})_{\mathrm{bonded}} \leftrightarrow (\mathrm{NH})_{\mathrm{free}} + (\mathrm{O{=}C})_{\mathrm{free}} \quad (1)$$

with an associated equilibrium constant K given by

$$K = \frac{[\mathrm{NH}]_{\mathrm{free}}[\mathrm{O{=}C}]_{\mathrm{free}}}{[\mathrm{NH\cdots O{=}C}]_{\mathrm{bonded}}} \quad (2)$$

The equilibrium constant K is related to the bonded amide fraction (X_b), to the enthalpy (ΔH), and to the entropy (ΔS) of HB breaking according to the following equation:[6]

$$\ln K = \ln\left[\frac{(1-X_b)^2}{X_b}\right] = -\frac{\Delta H}{R}\frac{1}{T} + \frac{\Delta S}{R} \quad (3)$$

where R is the gas constant. Experimentally, it has been found that the average strength of the amide hydrogen bonds in an amorphous polyamide decreases with an increase in temperature because of thermal expansion.[10] Thus, the number of HBs decreases with an increase in temperature. In agreement with the experimental results,[3,6] X_b decreases with an increase in temperature and changes from 0.81 at 300 K to 0.42 at 600 K.

A van't Hoff plot is built using X_b at different temperatures and eq 3 (Figure 6). The circles in Figure 6 show the experimental value for the semicrystalline PA-66.[3] The enthalpy ΔH of HB breaking can be obtained from the slope $-\Delta H/R$ of a linear fitting through the simulated points. Our values for the enthalpy and entropy of HB breaking in PA-66 are equal to 15.4 ± 0.6 kJ mol^{-1} and 21.7 ± 1.2 kJ K^{-1} mol^{-1}, respectively. ΔH is slightly lower than the values previously reported in the literature for a number of polyamides, which range from 29 to ~59 kJ mol^{-1}[3,5,6,35] (while ΔH for low-molecular weight amides ranges from 14.5 to 27 kJ mol^{-1}).[36] The dependence of ΔH on the HB criterion has been checked in our simulations, and we found similar values for ΔH at the different maximum values for H···O distances (0.25, 0.35, and 0.4 nm) and the minimum

values for $\theta_{N-H\cdots O}$ (90° and 150°). The discrepancy of ΔH with the experimental values is possibly related to the problem of interpreting the infrared spectral features observed in the N−H stretching region. As mentioned in the Introduction, the thermodynamic parameters associated with the HB dissociation obtained by infrared spectroscopy data can be strongly affected by errors. The usual practice of not taking into account the strong dependence of the absorption coefficient on the HB strength has indeed led to an overestimation of the fraction of free N−H groups and, in turn, to an overestimation of the enthalpy of HB breaking.[10] To this erroneous practice Skrovanek and co-workers[10] also ascribed the large discrepancy found between their experimental values of ΔH compared to those of their low-molecular weight analogues. However, the effect of the lower molecular weight of our model compared to the experimental one cannot be ruled out completely, and the presence of entanglements (as likely occur in the experimental samples) could increase the value of ΔH.

Dynamic Properties of Hydrogen Bonds. The dynamics of HBs in the bulk of PA-66 was investigated by calculating the structure relaxation time, the rate constant of HB breaking, and the average HB lifetime. We calculated these dynamical properties for HBs between amide groups in terms of two time correlation functions (TCFs), namely, the continuous HB time correlation function, $S(t)$, and the intermittent HB time correlation function, $C(t)$.[16,17,37] These TCFs are defined as

$$S(t) = \frac{\langle \delta h(0)\delta H(t)\rangle}{\langle \delta h(0)\delta H(0)\rangle} = \frac{\langle h(0)H(t)\rangle - \langle h\rangle\langle H\rangle}{\langle h\rangle - \langle h\rangle\langle H\rangle} \approx \frac{\langle h(0)H(t)\rangle}{\langle h\rangle} \quad (4)$$

and

$$C(t) = \frac{\langle \delta h(0)\delta h(t)\rangle}{\langle \delta h^2\rangle} = \frac{\langle h(0)h(t)\rangle - \langle h\rangle^2}{\langle h\rangle - \langle h\rangle^2} \approx \frac{\langle h(0)h(t)\rangle}{\langle h\rangle} \quad (5)$$

where the population variable $h(t)$ is unity when a particular hydrogen−oxygen pair is hydrogen bonded at time t, according to the definition, and zero otherwise. On the other hand, $H(t) = 1$ if the tagged O−H bond remains continuously hydrogen bonded during time duration t and zero otherwise. The brackets denote an average over all amide pairs and all starting times. The average number of HBs (N_{HB}) in a system of N amide groups is equal to the number of all pairs multiplied by the average value of the HB population operator ($\langle h\rangle$) [$N_{HB} = {}^1/_2 N(N - 1)\langle h\rangle$]. If N_{HB} (in a system containing N amide groups) has the same order of magnitude as N, then the approximations in eqs 4 and 5 follow because $\langle h\rangle \propto 1/N \approx 0$ when the number of amide groups is large.[38]

According to the definition, $C(t)$ describes the probability that a particular tagged HB is intact at time t, given it was intact at time zero, while $S(t)$ provides a definition of the lifetime of a tagged HB. The relaxation time of $C(t)$ is usually called the structural relaxation time (τ_R) of HBs, and the relaxation time of $S(t)$ describes the average HB lifetime (τ_{HB}). The long time behavior of $S(t)$ (which depends on the continuous presence of a HB) is strongly affected by short time fluctuations due to librational motion of the molecules and by the criterion for defining the HB. However, such fluctuations do not strongly affect the long time behavior of $C(t)$ (which does not depend on the continuous presence of a HB but allows for intermittent HBs). Thus, $S(t)$ is sensitive to the sampling frequency, and choosing a long time interval between sampled configurations corresponds to ignoring processes where a bond is broken for a short time and subsequently re-forms. To calculate $S(t)$ in our simulations, we sampled the configurations every 10 fs (shorter than the typical libration time, which could destroy a bond),[14] while $C(t)$ was obtained with time resolution of 10 ps.

Figure 7a shows the time correlation function $C(t)$ at different temperatures. At very short times, $C(t)$ decays rapidly due to librational motion. After the initial rapid decay, it remains relatively constant, especially at low temperatures: for temperatures below 400 K, the correlation function does not relax within the 20 ns, while for temperatures above 400 K, $C(t)$ decays very fast to zero. At all temperatures, $C(t)$ shows the presence of slow components at long times. Such slow long time decay cannot be described by a single-exponential function or by a stretched-exponential function.[13] To determine the relaxation times (τ_R), we fit the decay curves (Figure 7a) to three exponentials and extrapolated. The parameters for best fits along with the amplitude-weighted average τ_R for four temperatures are listed in Table. 1. As we can see in Table 1, we have an abrupt increase in the structural relaxation time as the glass transition temperature T_g (330 K) as calculated from our atomistic model[26] approaches.

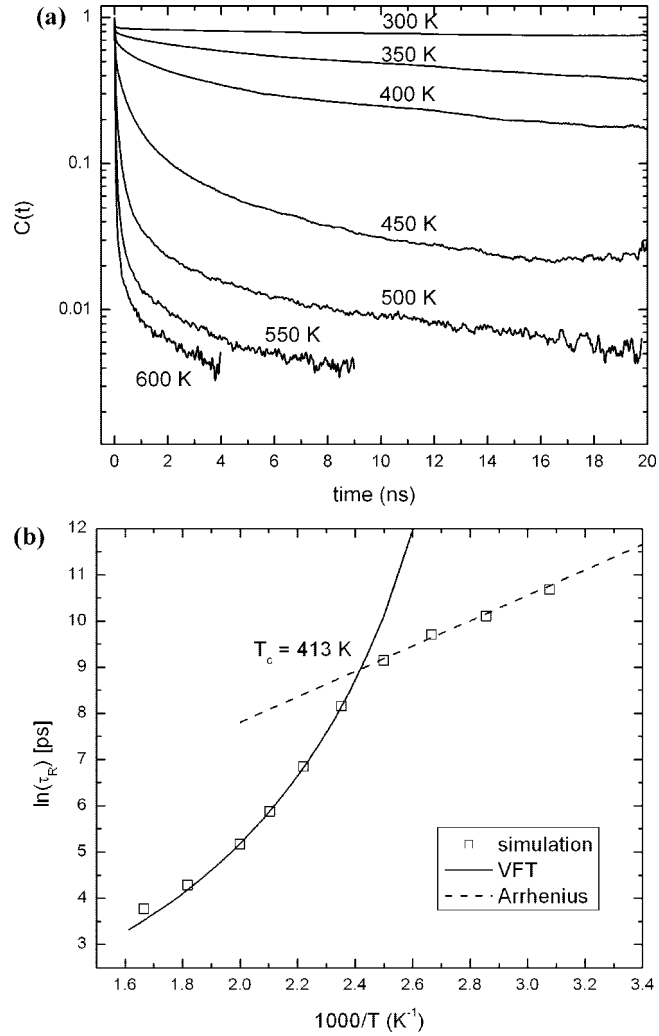

Figure 7. (a) Semilog plot of the structural time correlation function $C(t)$ for amide−amide hydrogen bonds at different temperatures. (b) Temperature dependence of structure relaxation time plotted for temperatures ranging between 300 and 600 K. The dashed line denotes a fit to an Arrhenius law at T <413 K and the solid line a fit to a Vogel−Fulcher−Tammann (VFT) law at $T \geq 413$ K. Error bars are smaller than the symbols.

To analyze the behavior of τ_R in PA-66 at different temperatures, we plotted the structural relaxation time in $\log(\tau_R)$ versus $1000/T$ in Figure 7b. At $T \geq 413$ K, τ_R can be fit well by the Vogel−Fulcher−Tammann (VFT) equation, $\tau_R \propto e^{AT_0/(T-T_0)}$, where $A = 3.36$ and $T_0 = 298.88$ K. The VFT fit deviates visibly from the data at $T \leq 413$ K, where one can see a sudden change in the slope of the $1/T$ dependence of $\log(\tau_R)$. The relaxation time τ_R at low temperatures can be fitted by the Arrhenius

Table 1. Multiexponential Fitting Parameters for the Oxygen−Hydrogen Intermittent [$C(t)$] and Continuous [$S(t)$] Hydrogen Bond Time Correlation Functions at 300, 400, 500, and 600 K

	$C(t)$			$S(t)$		
temp(K)	time constant (ps)	amplitude (%)	τ_R (ps)	time constant (ps)	amplitude (%)	τ_{HB} (ps)
300	201188.0	81.7	164550.0	2.5	37.4	1.2
	58.5	14.9		0.5	44.7	
	2453.7	3.2		0.1	16.9	
400	23449.3	37.7	9302.9	0.9	24.9	0.4
	11.2	31.9		0.3	52.4	
	1594.2	29.0		0.1	22.3	
500	2031.5	6.3	174.7	0.3	58.6	0.2
	5.4	57.6		0.1	20.6	
	118.3	36.0		0.1	20.9	
600	1834.0	1.7	43.1	0.3	14.3	0.1
	4.3	81.1		0.2	54.8	
	45.4	17.1		0.1	31.0	

equation ($\tau_R \propto e^{E_A/k_BT}$, with an activation energy E_A of 22.81 kJ mol^{-1}). Thus, with a decrease in temperature, the dependence of τ_R on temperature becomes weaker and shows a crossover between two different regimes at approximately $T_c = 413$ K (T_c is the crossover temperature between the VFT and Arrhenius fits). The presence of this crossover will be explained further below.

As mentioned in the Introduction, different kinds of glass-forming liquids can be classified according to the dependence of their transport properties (TPs), i.e., viscosity and self-diffusion coefficient, on temperature. The TPs in strong glass formers follow an Arrhenius type equation (TP $= Be^{A/T}$, with B and A being fitting parameters), while in the fragile glasses, they are described by the Vogel−Fulcher−Tammann (VFT) equation [TP $= Be^{AT_0/(T-T_0)}$, with B, A, and T_0 as fitting parameters]. Recent improvements in the mode-coupling theory (MCT) of the glass transition[39,40] predict the existence of a crossover of the dynamics at the molecular level, at some critical temperature, T_c, above T_g. Experiments and numerical theories have investigated several low-molecular weight and polymeric systems[41] to test the MCT predictions, and it has been found that the empirical equations such as the Arrhenius or VFT equation alone are not able to fit several types of TPs over a large range of temperatures; in particular, it has been found that the TPs show a crossover from VFT to Arrhenius behavior around T_c. Indeed, many dynamic properties of glass-forming liquids, such as the α and β relaxation processes,[42] the rotational and translational diffusion coefficients,[43] and the dielectric relaxation strength,[44] show qualitative changes at a temperature around T_c. Thus, there is much evidence that some qualitative changes occur in the dynamics of glass-forming systems in a small temperature range above T_g. It has also been noted in refs 45 and 46 that the ratio T_c/T_g correlates with the fragility of glass-forming systems: the higher the fragility, the lower value of T_c/T_g.

Since the presence of HB affects strongly the transport properties of materials,[12,47−49] we investigated the trend of the chain self-diffusion coefficient D [$6D = \lim_{t\to\infty} d/dt \langle |R(t) - R(0)|^2 \rangle$] with temperature to find a possible relation among the behavior of τ_R and TP. Figure 8 reports D calculated only in the rubber phase ($T \geq 350$ K) considering the T_g found in our simulations (330 K).[26] At 414 K, a transition from a VFT to an Arrhenius behavior is visible. This temperature agrees with the one calculated from the τ_R (413 K), and it corresponds to the experiment "softening temperature" (the temperature above which the system changes from viscous flow to plastic flow) reported for PA-66 which lies at 413 K.[50] Moreover, the ratio T_c/T_g in our system (≈1.25) is in the same range as experimental values found for polybutadiene (≈1.20),[51] polyisobutylene (≈1.35),[22] and polystyrene (≈1.14).[22] The presence of a crossover temperature in our simulations is also in agreement with the recent theoretical work of Baeurle and co-workers[18] on the glassy state of polymer materials. Their physical interpretation of the crossover temperature can be summarized as follows. If the system is cooled very slowly to a temperature slightly above T_g (i.e., T_c), the glass-forming polymer becomes trapped in a quasi-equilibrium state by undergoing a percolation transition of high-density clusters which leads to variations in the local monomer density and mobility. The formation of a continuous backbone between the high-density clusters restricts the polymer mobility below T_c, causing a sudden increase in viscosity. Developed starting from observations made on the stress relaxation experiments conducted with styrenic block copolymers,[52] this model is able to describe correctly their mechanical response.[18] In the case of our simulations, it is possible that the hydrogen-bonded amide groups (randomly distributed or organized in clusters) whose number increases, decreasing the simulation temperature, form at the crossover temperature a continuous backbone causing the deceleration of the structural relaxation time (Figure 7a) and of the self-diffusion coefficient (see Figure 8). Further investigations into the spatial organization of the HBs and their percolation within the model could confirm this picture.

To compare the variation of the diffusion coefficient and structure relaxation time with temperature, we normalized $1/D$ and τ_R by their respective values at 600 K. This normalization was done by shifting the curves in Figures 7b and 8 to their corresponding values at 0.00167 K^{-1} (Figure 9). We observe that there is a collapse of the two curves; thus, we conclude that both dynamic properties exhibit the same behavior at

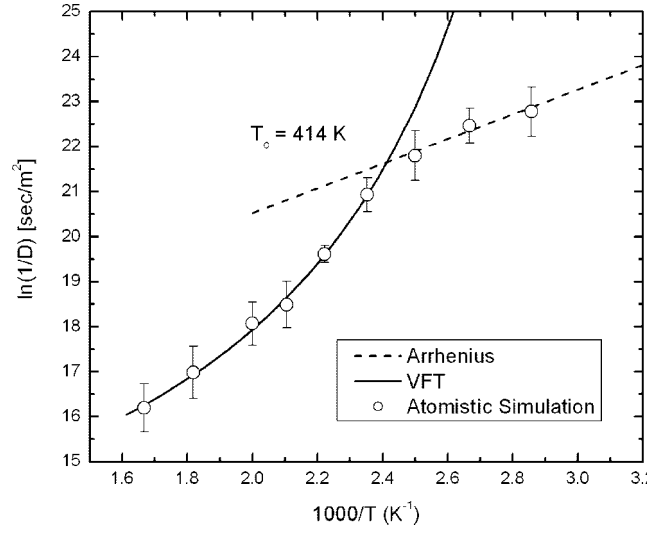

Figure 8. Temperature dependence of the chain self-diffusion coefficient plotted for temperatures above T_g (330 K). The dashed line denotes a fit to an Arrhenius law when $T < 414$ K and the solid line a fit to a Vogel−Fulcher−Tammann (VFT) law when $T \geq 414$ K.

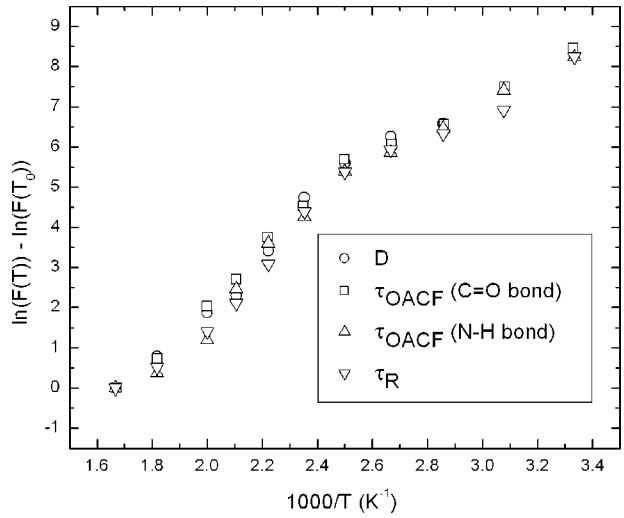

Figure 9. Normalization of the curves in Figures 7b and 8 and the time correlations from the orientational correlation function of C═O and N−H bonds by the corresponding values at 600 K (T_0). The function $F(T)$ corresponds to $1/D$, τ_R, and τ_{OACF} for C═O and N−H bonds.

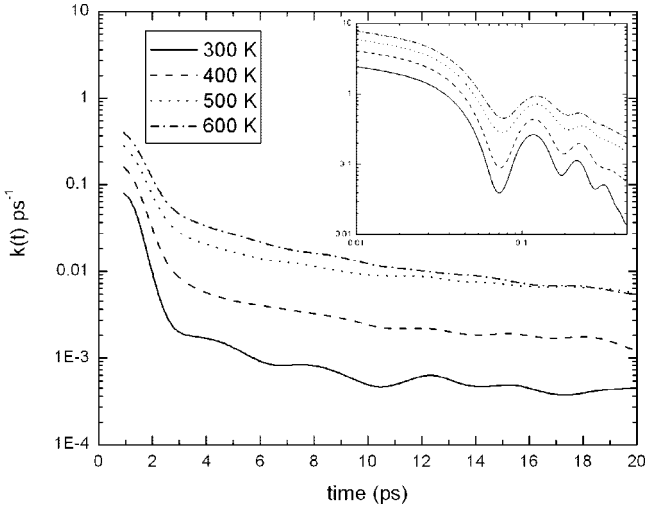

Figure 10. Reactive flux HB correlation function $k(t)$ at 300, 400, 500, and 600 K extracted from the atomistic simulations. The inset panel shows a log−log plot of the same function at short times.

different temperatures. In Figure 9, we also include the correlation times from the orientational correlation functions (τ_{OACF}) of C═O and N−H bonds which are shown in Figure 2. τ_{OACF} values are calculated in a same way as τ_R by fitting the orientational correlation functions (Figure 2) with three exponential functions. The normalization of the correlation times by the corresponding values at 600 K (Figure 9) shows that different dynamic properties of the system ($1/D$, τ_R, and τ_{OACF}) are coupled and follow the same behavior with temperature.

The rate of relaxation to equilibrium is characterized by the reactive flux HB correlation function, $k(t)$

$$k(t) = -\frac{dC(t)}{dt}$$

where $-k(t)$ is the rate of change of the HB population at time t. To study the variation of $k(t)$ at short times, we calculated the derivative of the intermittent HB correlation function $C(t)$ (eq 5) obtained with a time resolution of 1 ps (Figure 10). The $k(t)$ values determined from our simulation at four temperatures are shown in Figure 10. At short times, $k(t)$ quickly changes from its initial value. The angular restriction of the HB definition

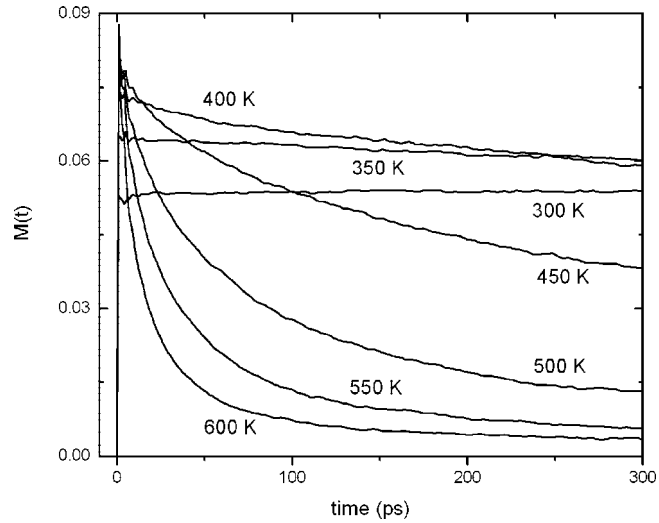

Figure 11. Time dependence probability that amide−amide HBs are broken, but they remain in the vicinity of each other.

makes it very sensitive to librational motion, which has a characteristic time of <0.1 ps. To gain a better view of the relaxation for a time scale of <1 ps, we used $C(t)$ with a time resolution of 10 fs (inset of Figure 10). At this time scale, the system undergoes several transitions from forming the HB to breaking the HB and the reactive flux shows a dip at $t \approx 0.07$ ps (see the inset of Figure 10). Thus, the dip is created by the pairs initially hydrogen bonded which are broken (by libration) but often re-form a HB. Beyond this transient period, $k(t)$ decays monotonically, and for times of >2 ps, it will not change much with time at different temperatures. As shown in Figure 10, the reactive flux function, $k(t)$, has a larger value for higher temperatures until 20 ps; however, there is a big difference between the $k(t)$ at 300 and 400 K, while the $k(t)$ has almost same value at long times for 500 and 600 K. These results show that temperature affects the rate of relaxation to equilibrium more at low temperatures than at high temperatures.

The dynamics of HBs between amide groups is strongly coupled to the diffusion of the molecules. Faster diffusion will result in faster HB relaxation and vice versa.[12] After a HB is broken, the amide groups can remain in the vicinity for some time before the bond is reformed or they diffuse away from each other. To study the effect of diffusion on the dynamics of HBs at different temperatures, we calculated the time correlation function[48,53]

$$M(t) = \frac{\langle h(0)[1-h(t)]H'(t)\rangle}{\langle h\rangle}$$

where $H'(t)$ is unity if the tagged pairs of hydrogen and oxygen are closer than 0.297 nm at time t and zero otherwise. In Figure 11, the relaxation of $M(t)$ at different temperatures is shown. As discussed before, we have a fragile-to-strong transition in the transport properties of the system at $T_c = 413$ K. This crossover can also be identified in the relaxation of $M(t)$. The figure shows that $M(t)$ is almost constant below 400 K, while it relaxes fast above 400 K. A low diffusion coefficient at temperatures below 400 K causes low mobility of the amide groups that remain in the vicinity of each other after the break of the HB, increasing the probability of re-forming it. Thus, $C(t)$ and $M(t)$ decay very slowly for low temperatures, while at high temperatures (above 400 K), they decay very fast since after the HB rupture the amide groups can diffuse easily away from each other.

In Figure 12a, we show the relaxation of the continuous HB time correlation function, $S(t)$, at different temperatures. As we

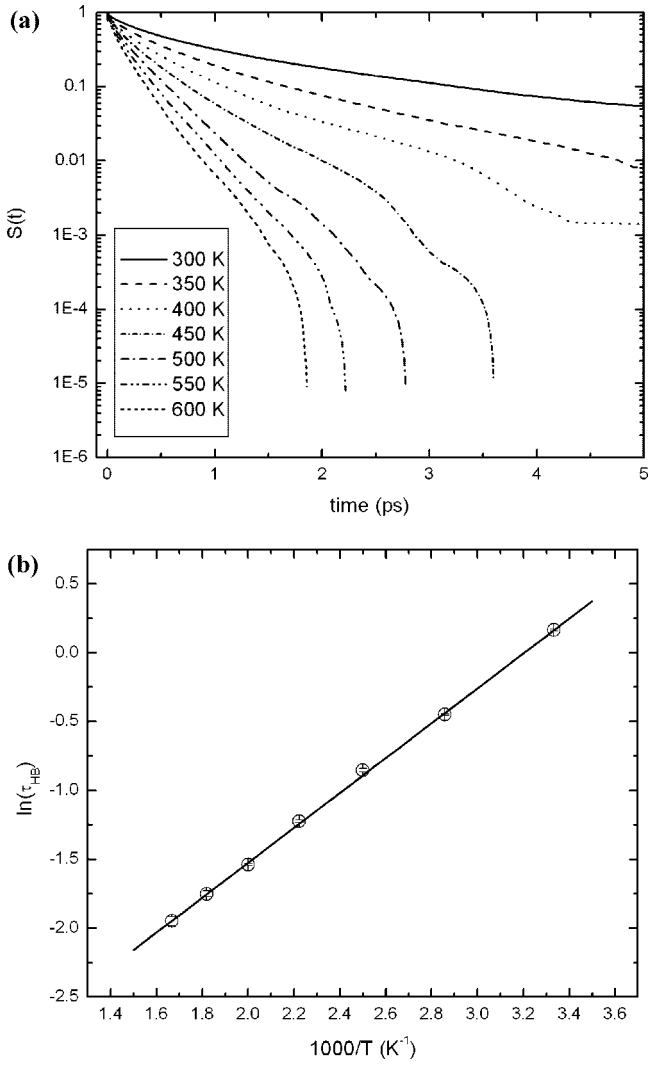

Figure 12. (a) Semilog plot of the time correlation function $S(t)$ for HB between oxygen and hydrogen of the amide groups at different temperatures. (b) Hydrogen bond lifetimes (τ_{HB}) obtained from $S(t)$. The line is a fit to the Arrhenius law.

find for intermittent HB the time correlation function [$C(t)$], $S(t)$ decays very fast at short times due to librational motion, but the correlation functions at different temperatures do not show a long time relaxation compared to $C(t)$. $S(t)$, like $C(t)$, can be fitted to a sum of three exponentials. The fitting parameters and the amplitude-weighted average HB lifetimes (τ_{HB}) for four temperatures are given in Table 1. The HB lifetime decreases with an increase in temperature, from 1.18 to 0.14 ps from 300 to 600 K. In Figure 12b, we display the variation of τ_{HB} in a semilog plot versus 1000/T. The figure shows that the mean HB lifetimes obtained from $S(t)$ follows an Arrhenius behavior at different temperatures ($\tau_{HB} \propto e^{E_A/k_BT}$) with an activation energy of 10.5 ± 0.5 kJ mol^{-1}. The activation energy associated with the hydrogen bond lifetime is interpreted as the energy required to break a HB via librational motion, a fast motion.[54] The Arrhenius behavior of τ_{HB} is in agreement with experimental results conducted with liquid water in different environments.[14,17,38,54−56]

Conclusions

We have analyzed the hydrogen bond dynamics in bulk polyamide-66 by means of molecular dynamics simulations. Our geometrical definition of the HB has led to a hydrogen bond enthalpy ΔH value that is in agreement with experimental data, especially with those measured for low-molecular weight amides. Following the time relaxation of several correlation functions, we have found that the global dynamics of unentangled polyamide-66 is governed by the relaxation of the hydrogen bond network formed among the amide groups. By looking at the behavior of the self-diffusion coefficient and the structural relaxation times, we identified a transition temperature (T_c) at ~413 K, and it corresponds to the experiment softening temperature reported for polyamide-66 which is 413 K.[50] Approaching T_c from above, the temperature dependence of these two dynamic variables changes continuously from VFT to Arrhenius behavior. Our simulation results confirm the most recent theoretical works[18,19] predicting an Arrhenius behavior of the diffusion coefficient in supercooled polymers and, in the case of polyamide-66, relate unequivocally the relaxation of the hydrogen bonds with the global dynamics of the polymer. According to the most recent glass theory,[18,19] the crossover temperature found in our simulations can be seen as the temperature at which the polymer melt is subjected to spatiotemporal fluctuations that lead to variations in the local mobility governed by the relaxation of the HBs. Our results have also confirmed that this transition temperature does not coincide with the glass transition one, but their ratio falls into the typical values found experimentally for other polymeric systems.

It must be noticed that in contrast, the hydrogen bond lifetimes (time to first rupture) governed by the local librational dynamics of the amide groups show an Arrhenius behavior over the whole temperature range.

In summary, we have shown that for unentangled polyamide-66 the continuous change in the temperature dependence of the diffusion coefficient from the VFT to Arrhenius form corresponds, at the molecular level, to a change in the hydrogen bond dynamics. This result shows that for polyamides the extrapolation of high-temperature properties to low temperatures is not reliable. The interpretation at the molecular level of the crossover transition found for PA-66 can help in understanding the physical aging process for other polymeric materials characterized by an extensive hydrogen bond network.

Acknowledgment. P.C. thanks the Alexander von Humboldt Foundation for a fellowship. This work has been supported by the Deutsche Forschungsgemeinschaft. We are thankful to the Hochschulrechenzentrum der Technische Universität Darmstadt for granting time on the IBM Regatta p575 machines (HHLR) located at TU Darmstadt, Darmstadt, Germany.

References and Notes

(1) Kohan, M. I. *Nylon Plastics Handbook*; Hanser Gardener: Cincinnati, 1995.
(2) Murthy, N. S. *J. Polym. Sci., Part B: Polym. Phys.* **2006**, *44*, 1763.
(3) Garcia, D.; Starkweather, H. W. *J. Polym. Sci., Polym. Phys. Ed.* **1985**, *23*, 537.
(4) Bessler, E.; Bier, G. *Makromol. Chem.* **1969**, *122*, 30.
(5) Trifan, D. S.; Terenzi, J. F. *J. Polym. Sci.* **1958**, *28*, 443.
(6) Schroeder, L. R.; Cooper, S. L. *J. Appl. Phys.* **1976**, *47*, 4310.
(7) Slichter, W. P. *J. Polym. Sci.* **1958**, *35*, 77.
(8) Xenopoulos, A.; Wunderlich, B.; Narten, A. H. *Macromolecules* **1993**, *26*, 1576.
(9) Lu, Y.; Zhang, G.; Feng, M.; Zhang, Y.; Yang, M.; Shen, D. *J. Polym. Sci., Part B: Polym. Phys.* **2003**, *41*, 2313.
(10) Skrovanek, D. J.; Howe, S. E.; Painter, P. C.; Coleman, M. M. *Macromolecules* **1985**, *18*, 1676.
(11) Skrovanek, D. J.; Painter, P. C.; Coleman, M. M. *Macromolecules* **1986**, *19*, 699.
(12) Luzar, A.; Chandler, D. *Phys. Rev. Lett.* **1996**, *76*, 928.
(13) Chanda, J.; Chakraborty, S.; Bandyopadhyay, S. *J. Phys. Chem. B* **2006**, *110*, 3791.
(14) Starr, F. W.; Nielsen, J. K.; Stanley, H. E. *Phys. Rev. Lett.* **1999**, *82*, 2294.
(15) Tamai, Y.; Tanaka, H. *Macromolecules* **1996**, *29*, 6761.

(16) Stillinger, F. H. *Adv. Chem. Phys.* **1975**, *31*, 1.
(17) Stillinger, F. H. *Science* **1980**, *209*, 451.
(18) Baeurle, S. A.; Hotta, A.; Gusev, A. A. *Polymer* **2006**, *47*, 6243.
(19) DiMarzio, E. A.; Yang, A. J. M. *J. Res. Natl. Inst. Stand. Technol.* **1997**, *102*, 135.
(20) Gibbs, J. H. *J. Chem. Phys.* **1956**, *25*, 185.
(21) Adam, G.; Gibbs, J. H. *J. Chem. Phys.* **1965**, *42*, 139.
(22) Kisliuk, A.; Mathers, R. T.; Sokolov, A. *J. Polym. Sci., Part B: Polym. Phys.* **2000**, *38*, 2785.
(23) O'Connell, P. A.; McKenna, G. B. *J. Chem. Phys.* **1999**, *110*, 11054.
(24) Gerardin, J.; Mohanty, S.; Mohanty, U. *J. Chem. Phys.* **2003**, *119*, 4473.
(25) Zang, Y.-H.; Carreau, P. J. *J. Appl. Phys. Sci.* **1991**, *42*, 1965.
(26) Goudeau, S.; Charlot, M.; Vergelati, C.; Müller-Plathe, F. *Macromolecules* **2004**, *37*, 8072.
(27) Berendsen, H. J. C.; Postma, J. P. M.; Gunsteren, W. F. v.; Nola, A.; Haak, J. R. *J. Chem. Phys.* **1984**, *81*, 3684.
(28) Ryckaert, J.-P.; Ciccotti, G.; Berendsen, H. J. C. *J. Comput. Phys.* **1977**, *23*, 327.
(29) Müller-Plathe, F.; Brown, D. *Comput. Phys. Commun.* **1991**, *78*, 77.
(30) Müller-Plathe, F. *Comput. Phys. Commun.* **1993**, *78*, 77.
(31) Bradbury, E. M.; Elliot, A. *Polymer* **1963**, *4*, 47.
(32) Viers, B. D. *Polymer Data Handbook*; Oxford University Press: New York, 1999.
(33) Savage, H. F. J.; Finney, J. L. *Nature* **1986**, *322*, 717.
(34) Lopez, C. F.; Nielsen, S. O.; Klien, M. L.; Moore, P. B. *J. Phys. Chem. B* **2004**, *108*, 6603.
(35) Hobza, P.; Mulder, F.; Sandorfy, C. *J. Am. Chem. Soc.* **1982**, *104*, 925.
(36) Pimentel, G. C.; McClellan, A. L. *The Hydrogen Bond*; W. H. Freeman and Co.: San Francisco, 1960.
(37) Rapaport, D. C. *Mol. Phys.* **1983**, *50*, 1151.
(38) Luzar, A. *Chem. Phys.* **2000**, *258*, 267.
(39) Götze, W.; Sjögren, L. *Rep. Prog. Phys.* **1992**, *55*, 241.
(40) Götze, W. *J. Phys.: Condens. Matter* **1999**, *11*, A1.
(41) Novikov, V. N.; Sokolov, A. P. *Phys. Rev. E* **2003**, *67*, 031507.
(42) Döss, A.; Paluch, M.; Sillescu, H.; Hinze, G. *Phys. Rev. Lett.* **2002**, *88*, 095701.
(43) Rössler, E. *Phys. Rev. Lett.* **1990**, *65*, 1595.
(44) Schönhals, A. *Europhys. Lett.* **2001**, *56*, 815.
(45) Rössler, E.; Sokolov, A. P.; Kisliuk, A.; Quitmann, D. *Phys. Rev. B* **1994**, *49*, 14967.
(46) Sokolov, P.; Kisliuk, A.; Quitmann, D.; Kudlik, A.; Rössler, E. *J. Non-Cryst. Solids* **1994**, *138*, 172.
(47) Luzar, A.; Chandler, D. *Nature* **1996**, *397*, 55.
(48) Xu, H.; Berne, B. J. *J. Phys. Chem. B* **2001**, *105*, 11929.
(49) Xu, H.; Stern, H. A.; Berne, B. J. *J. Phys. Chem. B* **2002**, *106*, 2622.
(50) http://www.lenzing.com/plastics/en/5750.jsp.
(51) Arbe, A.; Richter, D.; Colmenero, J.; Farago, B. *Phys. Rev. E* **1996**, *54*, 3853.
(52) Baeurle, S. A.; Hotta, A.; Gusev, A. A. *Polymer* **2005**, *46*, 4344.
(53) Paul, S.; Chandra, A. *Chem. Phys. Lett.* **2004**, *386*, 218.
(54) Chen, S.-H.; Teixeira, J. *Adv. Chem. Phys.* **1985**, *64*, 1.
(55) Conde, O.; Teixeira, J. *Mol. Phys.* **1984**, *53*, 951.
(56) Laenen, R.; Simeonidis, K.; Laubereau, A. *J. Chem. Phys.* **2002**, *112*, 8487.

MA8010685